scientific reports

Check for updates

OPEN

NLRP3 inflammasome inhibits mitophagy during the progression of temporal lobe epilepsy

Mengqian Wu[1], Cong Yu[1], Fuli Wen[2], Yunfei Li[1], Xu Zhang[1], Yinzhou Wang[1], Xiaoqian Chen[1]✉ & Xingyong Chen[1]✉

Epilepsy is a neurological disorder involving mitochondrial dysfunction and neuroinflammation. This study examines the relationship between NLRP3 inflammasome activation and mitophagy in the temporal lobe epilepsy, which has not been reported before. A pilocarpine-induced epileptic rat model was used to assess seizure activity and neuronal loss. Pyroptosis markers (NLRP3, cleaved Gasdermin D, IL-1β/IL-18), and autophagy/mitophagy activity (LC3B-II/I, BNIP3, TOMM20/LC3B colocalization) were analyzed via immunofluorescence, Western blot, and transmission electron microscopy. NLRP3 inhibitors and anti-IL-1β antibodies were administered to evaluate therapeutic effects. Epileptic rats exhibited progressive neuronal loss and seizure aggravation, correlating with NLRP3 inflammasome activation and pyroptosis. While general autophagy was upregulated, mitophagy was selectively impaired in the hippocampus. NLRP3 activation promoted IL-1β release, which suppressed mitophagy via PPTC7 upregulation. NLRP3 activation inhibitor (MCC950) and anti-IL-1β treatment restored mitophagy and reduced seizures. NLRP3 inflammasome-driven pyroptosis exacerbates epilepsy by impairing mitophagy activity via IL-1β/PPTC7. Targeted NLRP3 inhibition mitigates this cascade, offering a promising strategy for refractory epilepsy.

Keywords Temporal lobe epilepsy, Mitophagy, Autophagy, NLRP3 inflammasome, Pyroptosis

Epilepsy is a common and devastating neurological disorder characterized by recurrent seizures. The mechanism underlying epilepsy remains unclear. In recent years, increasing attention has been paid to the role of autophagy in the development of epilepsy. Some studies have suggested that impaired autophagy contributes to the onset of epilepsy[1,2]. Other studies have indicated that autophagy increases during brain damage induced by seizures[3–5]. Mitophagy is a selective form of autophagy that specifically clears damaged mitochondria[6], and it plays a crucial role in maintaining cellular health. Mitochondria are the organelles responsible for energy conversion and their dysfunction can lead to various diseases, including epilepsy[7,8]. Mitochondrial dysfunction can result in increased production of reactive oxygen species and impaired energy production, both of which can contribute to neuronal hyperexcitability, a key feature of epilepsy. Mitochondrial dysfunction is believed to be a part of the pathogenesis of epilepsy[9]. Numerous studies have confirmed that mitophagy is associated with many chronic neurological diseases, such as Parkinson's and Alzheimer's disease[10–13], few studies investigated the role of mitophagy in epilepsy[14,15]. Our previous study in human with temporal lobe epilepsy indicated that mitophagy is activated, but is insufficient to remove all of the damaged mitochondria in brain tissue samples from patients with refractory temporal lobe epilepsy[16]. However, the exact role of mitophagy in temporal lobe epilepsy has yet to be clearly delineated.

Impaired autophagy may lead to increased NLRP3 inflammasome activation, contributing to inflammatory responses and tissue damage. Some studies indicated that mitophagy can influence the activation of the nucleotide-binding oligomerization domain-like receptor family pyrin domain-containing 3 (NLRP3) inflammasome by regulating mitochondrial quality control[17]. When mitophagy is impaired or dysregulated, damaged mitochondria accumulate. This mitochondrial dysfunction can lead to the disruption of the mitochondrial membrane, resulting in the release of molecules from the intermembrane space, which may promote the activation of the NLRP3 pathway and trigger an inflammatory response. This phenomenon has been confirmed in some experimental models, such as in inflammatory diseases and neurodegenerative diseases[17–20].

[1]Department of Neurology, Fujian Provincial Hospital, Shengli Clinical Medical College of Fujian Medical University, Fuzhou University Affiliated Provincial Hospital, Fuzhou 350001, China. [2]Center for Experimental Research in Clinical Medicine, Fujian Provincial Hospital, Shengli Clinical Medical College of Fujian Medical University, Fuzhou University Affiliated Provincial Hospital, Fuzhou 350001, China. ✉email: chenxiaoqian-sl@qq.com; cxyong77@163.com

Pyroptosis is an inflammatory form of programmed cell death mediated by caspase-1. The triggering signals originate from various cytoplasmic sensor proteins, which promote the formation of the NLRP3 inflammasome complex, thereby activating caspase-1. Activated caspase-1 cleaves pro-interleukin-18 (pro-IL-18) and pro-interleukin-1β (pro-IL-1β) into their mature forms, IL-18 and IL-1β, and also cleaves Gasdermin D to form Gasdermin D-N-terminal fragments (Gasdermin D-NT). The latter forms pores in the cell membrane, leading to the release of inflammatory cytokines[21]. Pyroptosis is involved in the pathophysiology of various central nervous system disorders, such as intracerebral hemorrhage, Alzheimer's disease, and Parkinson's disease, and interventions targeting it may improve the prognosis of these diseases[22,23]. NLRP3 may be involved in the development of refractory temporal lobe epilepsy and pyroptosis has also been mentioned in epilepsy research[24–26]. However, the exact relationship between these processes and mitophagy remains unclear.

In the present study, we established a pilocarpine-induced epileptic rat model to investigate the effect of NLRP3 inflammasome activation on mitophagy in chronic temporal lobe epilepsy, with the aim of filling a gap in epilepsy research and providing new treatment strategies to address pressing clinical challenges.

Results

Hippocampal neuronal loss increases with seizure severity in the pilocarpine-Induced epileptic rat model

The temporal lobe epilepsy rat model induced by pilocarpine was successfully established (Fig. 1a). These rats exhibited spontaneous recurrent seizures (SRS) following an acute status epilepticus phase and progressed to the chronic phase. Seizure frequency and duration were recorded at 1, 2, and 3 months after the onset of SRS. The results demonstrated that, over time, the duration of daily seizures progressively increased, along with an increase in both the number and duration of seizures per month (Fig. 1b, c and e). Correspondingly, we observed neuronal loss in the cortex and hippocampus at 1, 2, and 3 months after the onset of seizures (EP-1 m, EP-2 m, and EP-3 m groups, respectively) using hematoxylin and eosin (HE) staining. Compared to the control group,

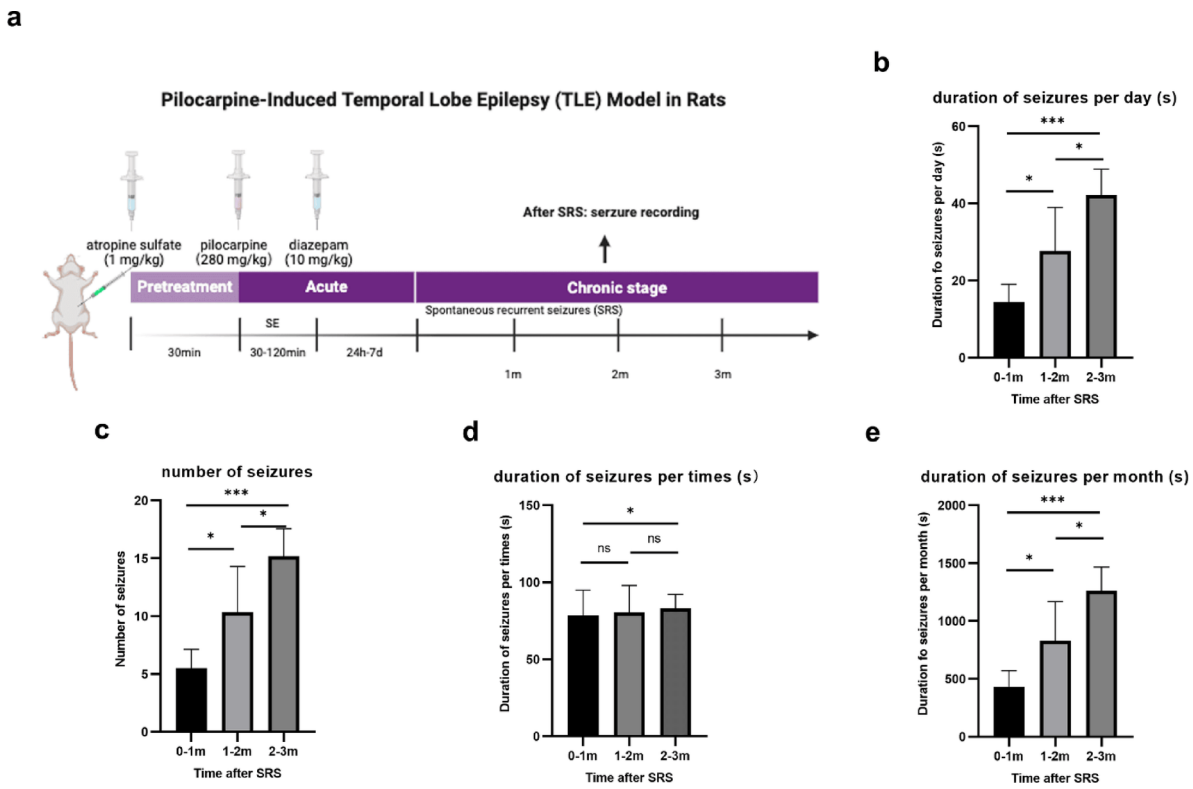

Fig. 1. Establishment of the pilocarpine-induced temporal lobe epilepsy rat model and comparison of rat epileptic behavioral results in different groups. (**a**) Pilocarpine-kindling progress. Following kindling, spontaneous recurrent seizures (SRS) were monitored for 3 months. Seizure activity was recorded and analyzed at three time points: 1, 2, and 3 months after SRS onset. Created on BioRender.com and licensed for publication. (**b**) Statistical results show that duration of seizures per day progressively increased ($n = 6$). (**c**) Statistical results show that total number of seizures per month progressively increased ($n = 6$). (**d**) Statistical results show that the duration of each seizure increased from the 0–1 month period to the 2–3 month period, while no significant difference was observed between the 1–2 month and 0–1 month periods, nor between the 1–2 month and 2–3 month periods ($n = 6$). (**e**) Statistical results show that total duration of seizures per month progressively increased ($n = 6$). Data are presented as means ± SEM (error bar) and compared using the two-sided Student's *t* test; $^{*}P < 0.05$; $^{**}P < 0.01$; and $^{***}P < 0.001$; ns, no significance.

a significant loss of neurons was observed in the epileptic (EP) groups, especially in hippocampus, and this loss became more pronounced with the increasing frequency and duration of seizures over time (Fig. 2a).

Pyroptosis is activated in the epileptic rat model, and inhibition of NLRP3 inflammasome activation alleviates seizure activity

Cell death can occur through various mechanisms, including necroptosis, apoptosis, and pyroptosis. In this study, we performed immunofluorescence staining to assess the expression of proteins related to necroptosis, apoptosis, and pyroptosis in the hippocampal tissue of pilocarpine-induced epileptic rats. Immunofluorescence analysis revealed that necroptosis marker proteins (pMLKL) and apoptosis marker proteins (cleaved caspase-3) were upregulated in the EP group compared to the control group, but no significant differences were noted between the three subgroups (EP-1 m, EP-2 m, EP-3 m) (Fig. 2b, c). In contrast, pyroptosis marker proteins (such as NLRP3, cleaved Gasdermin D, and cleaved IL-1β) were significantly elevated in the EP-1 m, EP-2 m, and EP-3 m groups compared to the control group, with inter-group differences also observed (Fig. 2b, c). Additionally, we also observed an increased release of IL-1β and IL-18 in the hippocampal tissue of epileptic rats, which progressively increased as the disease progressed (Fig. 2f, g). Furthermore, we assessed the activation of the NLRP3 inflammasome-induced pyroptosis pathway by Western blot and immunofluorescence. Compared to the control group, in both the cortex and hippocampus, protein levels of NLRP3, cleaved IL-1β, Gasdermin D-NT, and cleaved caspase-1 were significantly upregulated (Fig. 3a, b). These data indicate the activation of the NLRP3 inflammasome and its associated pyroptotic pathway in the pilocarpine-induced epileptic rat. And what's more, hippocampal neuronal loss in epileptic rats is predominantly driven by NLRP3 inflammasome-mediated pyroptosis, which exhibits progressive exacerbation during seizure development, unlike necroptosis or apoptosis which showed no temporal progression.

To further validate the role of NLRP3-dependent pyroptosis in epileptogenesis, we administered the pyroptosis inhibitor (MCC950), necroptosis inhibitor (GW806742X) and apoptosis inhibitor (zVAD-FMK) in pilocarpine-induced epileptic rat models. After 3 months of SRS, the MCC950 group exhibited significant reductions in both seizure frequency and duration, whereas neither GW806742X nor zVAD-FMK treatment showed significant effects (Fig. 2d, e). These results demonstrate that specific inhibition of NLRP3-dependent pyroptosis alleviates seizure severity, while no efficacy was observed with the necroptosis inhibitor or apoptosis inhibitor. These findings substantiate the critical role of the NLRP3 pathway in seizure-associated neuronal loss.

Activation of general autophagy in the pilocarpine-induced epileptic rat model

General autophagy is a tightly regulated process involving numerous molecules, with LC3B and p62 recognized as markers of autophagic activity. The process involves the conversion of LC3B-I to LC3B-II and its subsequent binding to p62 during autophagosome formation[27–29]. Western blot analysis revealed that in the hippocampus and temporal cortex of epileptic rats, the LC3B-II/I ratio was significantly increased while p62 expression was decreased compared to controls (Fig. 4a). Immunofluorescence analysis (Fig. 4c) consistently showed enhanced LC3B fluorescence intensity and reduced p62 expression in the epileptic group. Furthermore, we also observed RNA level of the markers of general autophagy including Beclin1, Atg5, Atg7, and Atg12, which were significantly elevated in epileptic rats compared to controls (Fig. 4b), especially in hippocampus, suggesting enhanced autophagic initiation in these regions. These findings collectively indicate general autophagy activation in the pilocarpine-induced epileptic rat model.

Impaired mitophagy and mitochondrial damage in the hippocampus of epileptic rats

We conducted co-localization analysis of TOMM20-labeled mitochondria and LC3B-labeled autophagosomes in the hippocampus and temporal lobe cortex of rats. Mitophagosome formation was indicated by the yellow fluorescence overlay of TOMM20 and LC3B. As depicted in Fig. 5a-c, an increase in mitophagosomes was observed in the cortex of the EP group compared to the control group, but no such increase was observed in the hippocampus. These results suggest that mitophagy is activated in the temporal lobe cortex of epileptic rats, while it may be inhibited in the hippocampus. At the same time, ultrastructural changes in the temporal cortex and hippocampus were examined using transmission electron microscopy. In the control group, mitochondria exhibited normal morphology with well-defined mitochondrial cristae (Fig. 5d). No double-membrane autophagosomes were detected. However, in the EP group, mitochondrial swelling and disrupted cristae were evident, with some mitochondria showing cristae disappearance, matrix cavitation, and intramitochondrial vacuoles (Fig. 5d). Mitochondria engulfed by double-membrane structures were observed, indicating the occurrence of mitophagy (green arrows). We quantified the damaged mitochondria in the cortex and hippocampus of rats. We found a significant increase in damaged mitochondria in the hippocampus of the EP group (Fig. 5d). In the cortical neurons, mitochondrial fragmentation was observed—specifically the loss of elongated, filamentous mitochondria and the appearance of round, fragmented mitochondria, which represents an intermediate step prior to mitochondrial packaging into autophagosomes and subsequent clearance. In conjunction with the co-localization analysis results, these damaged mitochondria were about to be cleared through mitophagy. However, in the hippocampus of epileptic rat, where mitochondrial damage was more severe, no significant increase in co-localized positive signals was observed, suggesting that mitophagy is impaired and insufficient to clear the damaged mitochondria. We then assessed the expression of mitophagy-related proteins in the mitochondrial fraction of the hippocampus from rats using Western blot analysis. In accordance with this, the expression of BNIP3 (a receptor involved in mitophagy) in EP group was decreased (Fig. 5f).

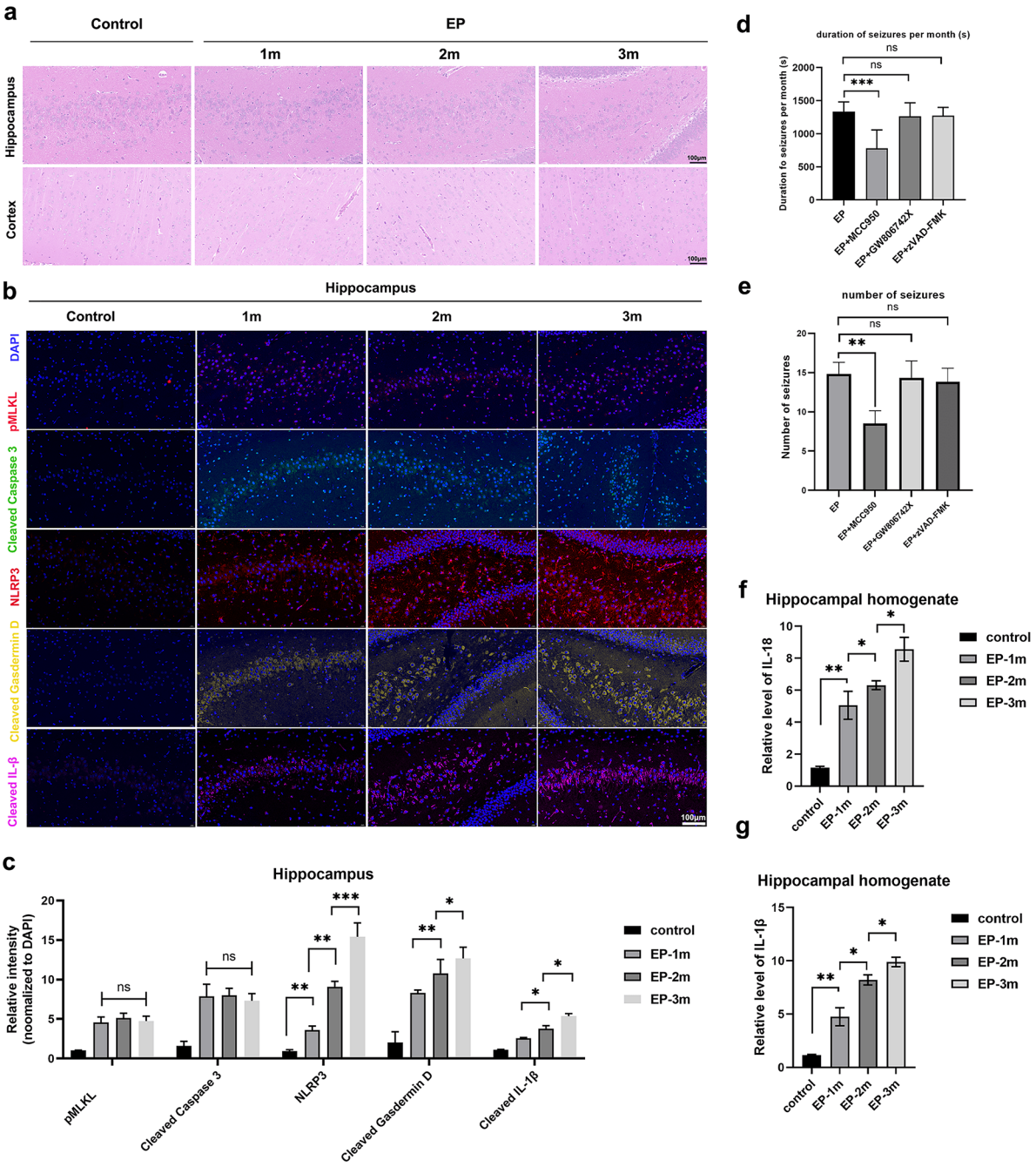

Fig. 2. Activation of pyroptosis in the epileptic rat model and the effect of NLRP3 inflammasome inhibition on seizure activity. (**a**) Representative Hematoxylin and Eosin staining images of hippocampus and cortex in control group and EP group; Scale bar: 100 μm. (**b**) Representative immunofluorescence images of necroptosis marker (pMLKL, red), apoptosis marker (cleaved caspase3, green), pyroptosis markers (NLRP3, red; cleaved Gasdermin D, yellow; cleaved IL-1β, purple) and DAPI (blue) in the hippocampus of rats; Scale bar: 100 μm. (**c**) Fluorescence intensity of pMLKL, cleaved caspase-3, NLRP3, cleaved Gasdermin D and cleaved IL-1β in the hippocampus of rats ($n = 3$). (**d**,**e**) Total duration of seizures per month and total number of seizures per month in EP group and treatment groups ($n = 3$). The inhibitors MCC950 (1 mg/kg, iv, twice a week for 3 month, a NLRP3 activation inhibitor), GW806742X (0.2 mg/kg, iv, three times a week for 3 month, a necroptosis inhibitor), and zVAD-FMK (3 mg/kg, iv, twice a week for 3 month, a apoptosis inhibitor) were applied. (**f**,**g**) The level of IL-1β and IL-18 in the hippocampus of rats detected by ELISA ($n = 3$). EP group: the epileptic model rat group; 1 m, 2 m, and 3 m represent at 1, 2, and 3 months after the onset of spontaneous recurrent seizures, respectively. Unless specified otherwise, the data are presented as means ± SEM (error bar) and compared using the two-sided Student's t test; $^{*}P < 0.05$; $^{**}P < 0.01$; and $^{***}P < 0.001$; ns, no significance.

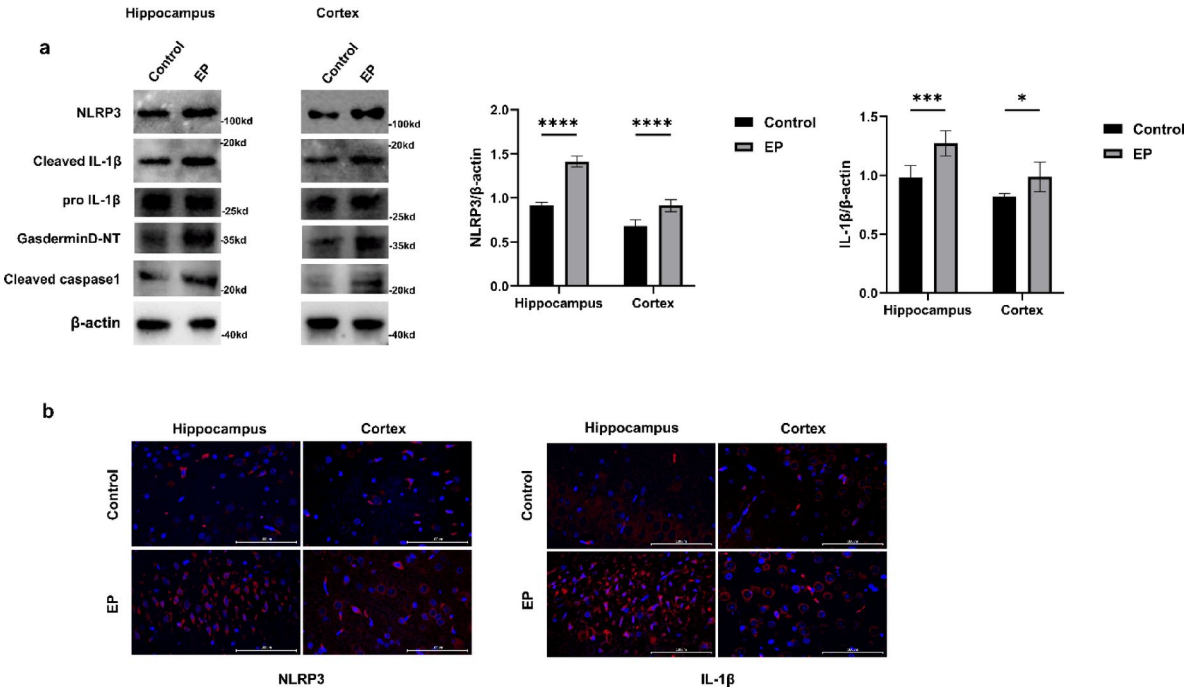

Fig. 3. NLRP3 inflammasome-induced pyroptosis activation in pilocarpine-induced epileptic rats. (**a**) Western blot analysis of NLRP3, cleaved IL-1β, pro IL-1β, Gasdermin D-NT, cleaved caspase-1 in the hippocampus and temporal lobe cortex of the control group and epileptic (EP) rat group. The gels of different group (Hippocampus group and cortex group) were not cropped in the same gel. (**b**) Immunofluorescence staining of NLRP3 and IL-1β in the hippocampus and temporal lobe cortex showed increased fluorescence intensity in the EP group. Scale bar for fluorescence images: 100 μm. Unless specified otherwise, the data are presented as means ± SEM (error bar) and compared using the two-sided Student's t test; * $p < 0.05$, ** $p < 0.01$, *** $p < 0.001$, **** $p < 0.0001$.

Activation of NLRP3 inflammasome promotes IL-1β release and inhibits mitophagy, aggravating seizures in pilocarpine-induced epileptic rats

The NLRP3 inflammasome, an innate immune signaling receptor, contributes to the pathogenesis of common non-infectious diseases by triggering potent inflammatory cytokines[30]. As mentioned earlier, our findings indicate heightened activation of the NLRP3 inflammasome in epileptic rats. Therefore, we further inhibited NLRP3 activation or the release of IL-1β from pyroptosis, both of which significantly reduced seizure frequency (Fig. 5e). We propose that the activation of NLRP3 and the release of IL-1β during pyroptosis play a crucial role in inducing mitophagy impairment. To investigate the effect of pyroptosis on mitochondria, we isolated the mitochondria and examined the impact of pyroptosis on mitochondrial function. Consistent with reports of gasdermin D-mediated mitochondrial permeabilization[31], our mitochondrial Western blot analysis showed cleaved Gasdermin D accumulation in the mitochondria, and BNIP3 degradation was significantly enhanced. These effects were reversed upon inhibition of NLRP3 activation or IL-1β release (Fig. 5f). Our data suggest that NLRP3 activation and IL-1β release are associated with PPTC7 upregulation, which leads to BNIP3 degradation and results in impaired mitophagy. PPTC7 transcription was upregulated in the EP group (Fig. 5g). Previous studies have reported PPTC7 as a negative regulator of BNIP3-mediated mitophagy[32]. In pyroptosis inhibitor (MCC950) and anti-IL-1β treated rats, we observed decreased PPTC7 expression (Fig. 5g). These results suggest that, in pilocarpine-induced epileptic rats, NLRP3 inflammasome activation disrupts mitochondria via Gasdermin D and promotes IL-1β-mediated PPTC7 upregulation, inhibiting mitophagy.

Discussion

The pathophysiological mechanisms of epilepsy are complex, which complicates its treatment and leads to difficulties in pharmacotherapy. Approximately 30% of patients continue to experience frequent seizures despite current antiepileptic drug treatments[33]. In this study, we utilized a pilocarpine-induced rat epileptic model to explore the impact of NLRP3 inflammasome activation on mitophagy in epilepsy. We observed that as the severity of seizures increased in the epileptic rats, there was a significant loss of neurons, with neuronal loss primarily mediated by NLRP3 inflammasome-induced pyroptosis. Along with the substantial activation of the NLRP3 inflammasome, mitophagy was insufficient, accompanied by severe mitochondrial damage. Our findings demonstrate that in the epileptic rat model, the activation of the NLRP3 inflammasome and the resulting IL-1β suppression of mitophagy occurs through the upregulation of the mitophagy-inhibitory PPTC7. This study further elucidates the regulatory role of NLRP3 inflammasome activation in mitophagy in epilepsy,

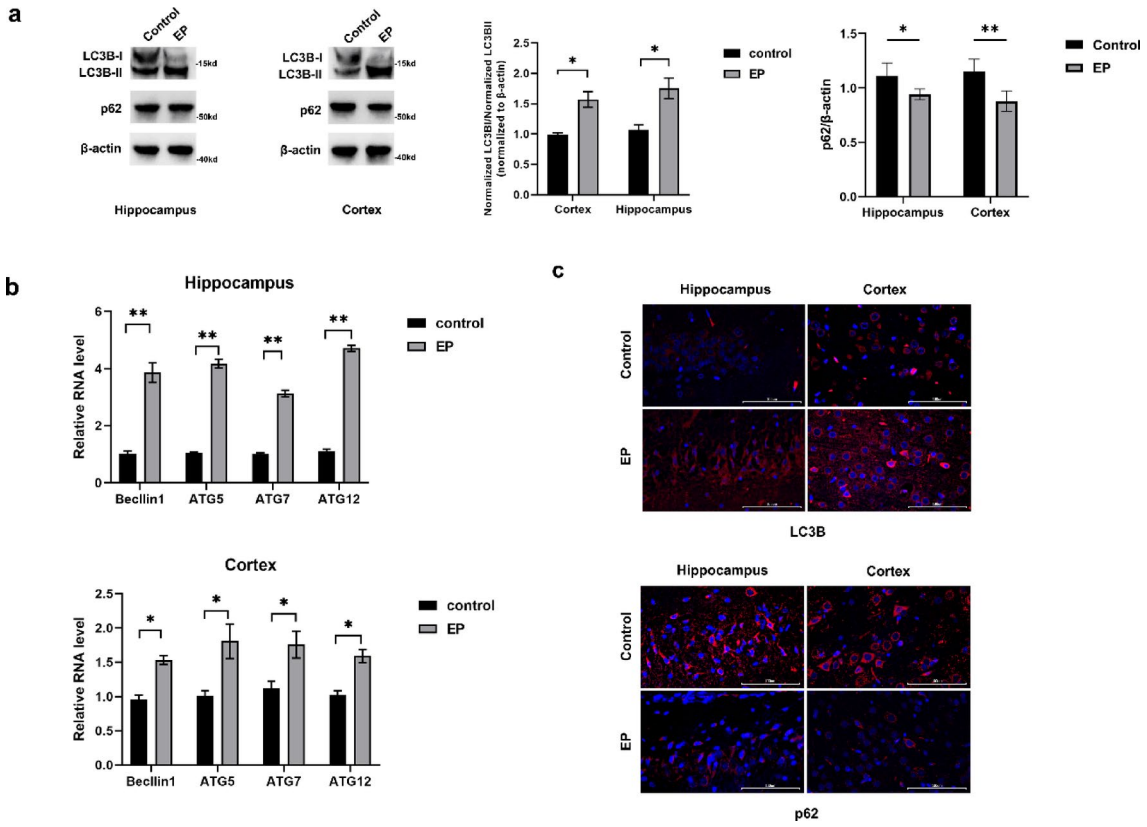

Fig. 4. Activation of general autophagy in the pilocarpine-induced epileptic rat model. (**a**) Western blot analysis of LC3B-II/I and p62 proteins in the hippocampus and temporal lobe cortex of the control group and epileptic (EP) rat group. The gels of different group (Hippocampus group and cortex group) were not cropped in the same gel. (**b**) Ralative RNA level of Beclin1, ATG5, ATG7, ATG12 in the hippocampus and temporal lobe cortex of the control group and epileptic (EP) rat group group ($n = 3$). (**c**) Immunofluorescence staining of LC3B and p62 in the hippocampus and temporal lobe cortex. Scale bar for fluorescence images: 100 μm. Unless specified otherwise, the data are presented as means ± SEM (error bar) and compared using the two-sided Student's t test; * $p < 0.05$, ** $p < 0.01$, *** $p < 0.001$, **** $p < 0.0001$.

a relationship not previously reported. This research supports the potential of NLRP3 inflammasome inhibitor and anti-IL-1β as promising therapeutic strategies for epilepsy, which alleviated seizure frequency in the rats.

The pilocarpine-induced epileptic rat model is widely recognized as an experimental model for temporal lobe epilepsy[34]. After establishing this model, we further monitored epileptic seizures and neuronal loss. We found that, as the frequency of spontaneous seizures increased and the duration of seizures prolonged, neuronal loss became more pronounced. These findings are consistent with previous studies[35].

As neuronal loss, mainly in the hippocampus, was observed in the epileptic model, we further investigated the types of cell death, including apoptosis, necroptosis, and pyroptosis, using immunofluorescence and Western blotting. We observed an increase in pyroptosis and activation of the NLRP3 inflammasome, marked by elevated levels of NLRP3, cleaved Gasdermin D, cleaved caspase-1 and cleaved IL-1β. NLRP3 inflammasome-mediated pyroptosis was identified as the primary form of neuronal loss during epilepsy progression. Pyroptosis is an inflammatory form of programmed cell death in which the NLRP3 inflammasome mediates the activation of pro-caspase-1, leading to the cleavage of Gasdermin D. This activation results in the formation of Gasdermin D-NT, which can puncture the cell membrane, releasing IL-1β and IL-18 through these pores, disrupting cellular homeostasis and resulting in cell death[36]. In our epileptic rat model, we also observed the release of these two cytokines, further emphasizing the significant role of NLRP3 inflammasome-mediated pyroptosis in epilepsy. Previous studies have demonstrated its involvement in the pathophysiology of epilepsy[24,25]. Therefore, NLRP3 inflammasome-mediated pyroptosis holds great potential as a target for the development of innovative therapies for epilepsy.

Interestingly, in the pilocarpine-induced epileptic rat model, we observed enhanced autophagic activity, but mitophagy was inhibited in the hippocampus, with a noticeable accumulation of severely damaged mitochondria. Previous studies have reported the critical role of autophagy in neurological disorders, such as Alzheimer's disease[11–13]. Recent research has highlighted the link between dysregulated autophagy and epilepsy[37–39], with limited studies suggesting that impaired mitophagy may exacerbate neuronal damage and seizure recurrence[16,40,41]. In this study, we observed a significant increase in the LC3B-II/LC3B-I ratio in the epileptic rats, indicating enhanced initiation of general autophagy[42] and, along with the reduction in p62, suggesting

effective downstream autophagic flux with smooth fusion of lysosomes and phagosomes[43–46]. Furthermore, in the hippocampal region of the epileptic rat model, the mitophagy marker BNIP3 was decreased, and fewer co-localization points of LC3B with TOMM20 were observed by immunofluorescence, indicating that mitophagy was impaired in the hippocampus. Transmission electron microscopy revealed a significant accumulation of damaged mitochondria, indicating that mitophagy was insufficient to clear the severely damaged mitochondria, reflecting a dysfunction in the mitophagy process in the hippocampus. Prolonged seizures have been reported to cause mitochondrial dysfunction and increased oxidative stress in the hippocampus, contributing to subsequent epileptogenesis[7,8]. This mitochondrial damage impairs ATP production and disrupts neuronal metabolism, leading to neurological complications such as recurrent seizures[47]. Recent studies have shown a complex relationship between mitophagy and pyroptosis in other disease contexts, and the prevailing view is that mitophagy and pyroptosis are negatively regulated through a feedback mechanism[48–50]. Activation of the inflammasome triggers caspase-1 activation, which inhibits mitophagy and further exacerbates mitochondrial damage[48]. We thus further investigated how pyroptosis regulates mitophagy and mitochondrial damage in the epileptic model.

We observed an increased localization of cleaved Gasdermin D in the mitochondria through Western blot analysis, suggesting that more pores were formed, potentially disrupting mitochondrial integrity. Pyroptosis, mediated by the activation of the NLRP3 inflammasome, led to elevated levels of IL-1β. The release of IL-1β, in turn, was associated with an upregulation of the mitophagy-inhibiting molecule PPTC7, which further contributed to mitochondrial impairment. A similar phenomenon has been observed in other studies[51]. Furthermore, we have tested the effects of anti-IL-1β and NLRP3 inflammasome inhibitors (MCC950) in the epileptic model, all of which alleviated the frequency of seizures to some extent. These results suggest that targeting IL-1β or inhibiting NLRP3 inflammasome activation may reduce seizure activity. The application of these treatments in humans, as well as their potential side effects, warrants further investigation. This highlights the potential of targeting pyroptosis as a novel and promising therapeutic approach for controlling epilepsy.

This study has several limitations. First, it relies solely on a pilocarpine-induced rat model, which may not fully replicate human epileptogenesis. Further studies using in vitro systems and other epilepsy models are needed for broader relevance. Second, while NLRP3 inflammasome activation and pyroptosis were observed, the exact upstream triggers and downstream effects remain unclear due to the complexity of chronic epilepsy and the brain. Lastly, the potential effects of confounding factors such as stress and inflammation on mitophagy markers have not been fully elucidated, as these factors are complex and may influence the interpretation of the results. This remains a significant challenge in the current academic field.

Conclusion: Our study highlights the relationship between NLRP3 inflammasome-mediated pyroptosis and mitophagy in the temporal lobe epilepsy rat model. We show that NLRP3 inflammasome activation and elevated IL-1β levels inhibit mitophagy by upregulating PPTC7. Further investigation is needed to clarify the mechanisms underlying mitophagy and NLRP3 inflammasome signaling in temporal lobe epilepsy.

Methods

Establishment of the experimental animal model

Male Sprague-Dawley rats (210–260 g) aged 6–8 weeks were purchased from the Shanghai Laboratory Animal Center, Chinese Academy of Science (license No. SYXK (Min) 2023-0005) and raised under standard conditions. The animal study was approved by the Animal Ethics Committee of Fujian Provincial Hospital, and all experimental procedures were performed according to the National Institutes of Health Guide for the Care and Use of Laboratory Animals. The authors complied with the ARRIVE guidelines.

Rats were randomly divided into the epileptic group and the control group. Rats in the epileptic group received intraperitoneal injections of 1 mg/kg of atropine sulfate 30 min before pilocarpine treatment (280 mg/kg; i.p.). Rats in the control group were injected with an equal volume of saline instead of pilocarpine. Within ten to forty-five minutes following pilocarpine injection, the rats exhibited generalized clonic-tonic seizures, progressing to continuous convulsive activity, known as status epilepticus. Status epilepticus persisted for 120 min before being terminated by intraperitoneal injection of diazepam (10 mg/kg). Rats surviving status epilepticus typically manifest spontaneous recurrent seizures (i.e., epilepsy) within days to weeks and continue to experience spontaneous seizures for several weeks[47,52], thereby establishing this model of temporal lobe epilepsy[53]. This model replicates the typical histopathological changes and spontaneous chronic seizures observed in patients with temporal lobe epilepsy. Behavioral seizures were graded according to Racine stages: stage 1, immobility, eye closure, twitching of vibrissae, and facial clonus; stage 2, head nodding; stage 3, clonus of one forelimb; stage 4, rearing, often accompanied by bilateral forelimb clonus; and stage 5, rearing and falling[54]. Video cameras were employed to monitor the behaviors of rats. At 1, 2, and 3 months after the rats exhibited spontaneous recurrent seizures, seizure number, seizure intensity, and seizure duration were documented. Seizure duration was defined as the period from the onset of limbic seizures (stages 1–2) until the end of the seizure, when rats resumed unrestricted movement. All rats were anesthetized with 2–3% isoflurane. Following induction of anesthesia, the animals were euthanized by cervical dislocation and perfused with phosphate-buffered saline.

Transmission electron microscopy

The hippocampus and temporal cortex of rats were dissected and cut into small specimens (approximately 1 mm thick), which were immediately immersed in a solution of paraformaldehyde and glutaraldehyde (in a 1:10 ratio) within 1–2 min of isolation. Subsequently, these samples were post-fixed in 1% osmium tetroxide, dehydrated using a series of graded ethanol solutions, and embedded using an 812 Embedding kit following standard protocols. Transmission electron microscopy images were captured using a JEM-1400 transmission electron microscope (JEOL Ltd.).

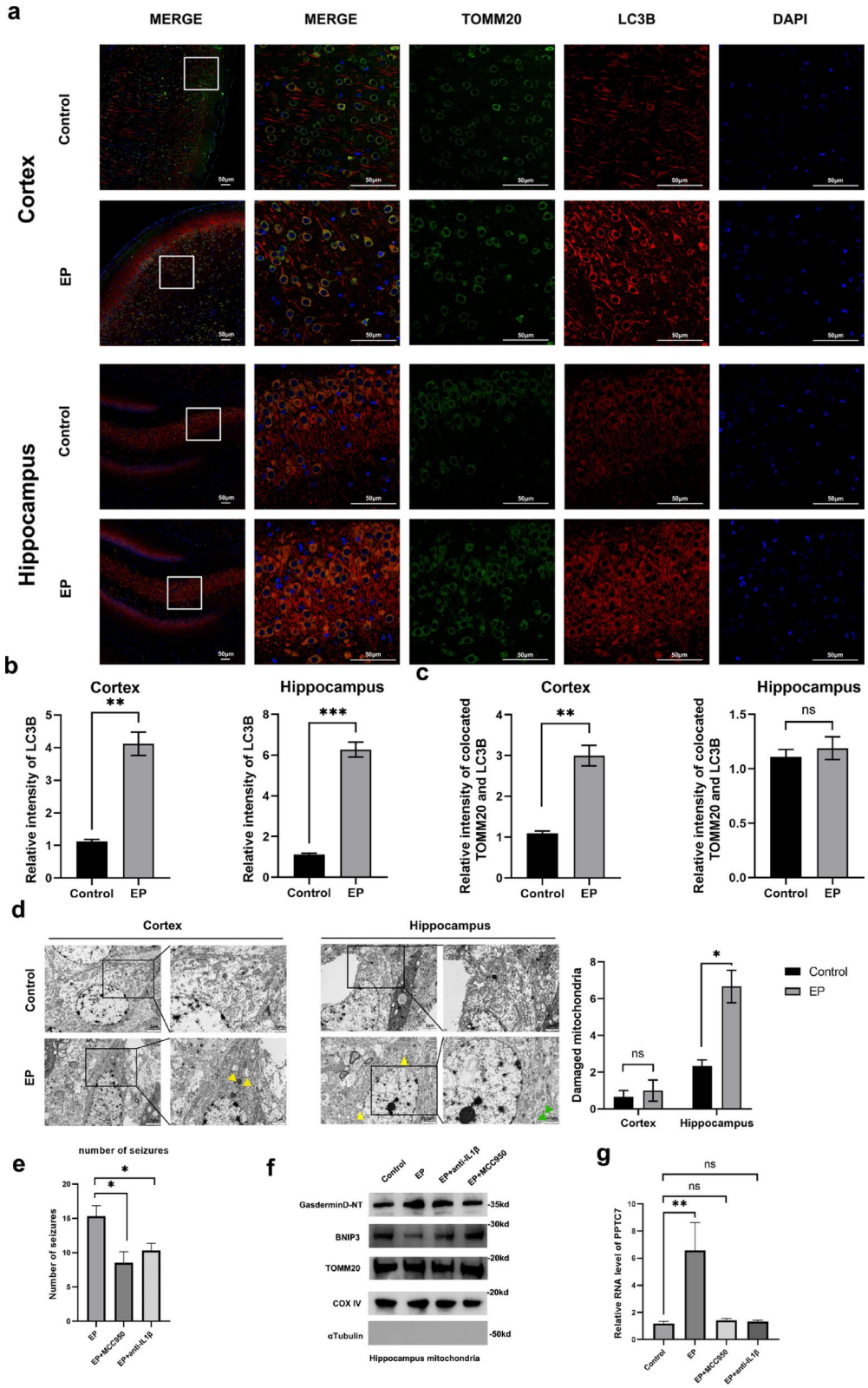

Each sample randomly selected five fields of view, and photographs were taken at the same magnification level. Mitochondrial impairment was identified by pathological ultrastructure changes, including swelling, cavitation of the matrix, disruption of cristae, and the appearance of intramitochondrial vacuoles[37,38,55,56]. Quantitative analysis of the degree of mitochondrial damage in the hippocampus and the temporal lobe cortex was performed. One randomly selected section of each specimen was photographed at × 25,000 magnification. Next, we randomly selected five visual fields within each section. The total number of severely damaged, slightly damaged, and intact mitochondria in the resulting TEM fields was calculated, to obtain a representative sample of the damage to mitochondria in the hippocampus or the temporal lobe cortex of rats. Early autophagosomes

◀**Fig. 5**. NLRP3 inflammasome activation inhibits mitophagy and modulates seizure activity in pilocarpine-induced epileptic rats. (**a**) The hippocampus and temporal lobe cortex of rats were double immunofluorescence stained for TOMM20-labeled mitochondria (green) and LC3B-labeled autophagosomes (red). Nuclei were stained with DAPI (blue). Enlarged views of areas within the white boxes are shown on the right. Scale bar: 50 μm. (**b**) Fluorescence intensity of LC3B in the hippocampus and temporal lobe cortex of rats ($n = 3$). (**c**) Colocalization fluorescence intensity of TOMM20 and LC3B in the hippocampus and temporal lobe cortex of rats ($n = 3$). (**d**) Representative transmission electron microscopy image of the temporal cortex and hippocampus showing varying degrees of mitochondrial damage (yellow arrows) in the rat. Green arrows indicate the occurrence of mitophagy in the epileptic (EP) group. Quantitative analysis revealed that damaged mitochondria in the hippocampus of the EP group were significantly higher than in the control group. (**e**) Number of seizures per month in EP group and treatment groups ($n = 3$). The inhibitors MCC950, anti-IL -1β were applied. (**f**) Western blot analysis of Gasdermin D-NT, BNIP3, TOMM20, and COX IV in the hippocampal mitochondria of the control group, EP group, and treatment group. (**g**) Relative RNA level of the mitophagy-inhibiting molecule PPTC7 in the control group, EP group, and treatment group ($n = 3$). Protein levels were quantified using Image J software. Unless specified otherwise, the data are presented as means ± SEM (error bar) and compared using the two-sided Student's t test; $^{*}P < 0.05$; $^{**}P < 0.01$; and $^{***}P < 0.001$; ns, no significance.

were recognized by a smooth, ribosome-free double membrane enveloping organelles such as mitochondria (known as mitophagy), vesicles, or other cytoplasmic material. Late autophagosomes or autophagolysosomes were distinguished by a double membrane fused into a single membrane[39,57].

Isolation of mitochondria from brain tissue

The brain tissues of rats were carefully dissected. Mitochondria were isolated using a commercial mitochondrial isolation kit, following previously established protocols[58]. In brief, the brain tissue samples were washed twice with 1× PBS and then homogenized in a designated isolation buffer. The homogenates were centrifuged at 1000×g for 5 min at 4 °C. The resulting supernatants were further centrifuged at 10,000×g for 20 min at 4 °C to collect the mitochondrial pellets. These pellets were then resuspended in PBS, as previously described[59].

Western blot analysis

Protein samples extracted from the hippocampus and temporal cortex were separated by sodium dodecyl sulfate-polyacrylamide gel electrophoresis (SDS-PAGE) using a 10% polyacrylamide gel, with the separation process performed in a running buffer containing 25 mM Tris, 192 mM Glycine, and 0.1% SDS (pH 8.3). The proteins were then transferred onto a polyvinylidene difluoride (PVDF) membrane (Millipore, Billerica, MA, USA) using a transfer buffer consisting of 25 mM Tris, 192 mM Glycine, and 20% methanol (pH 8.3). The membrane was blocked with 5% skim milk for 60 min and subsequently incubated with primary antibodies overnight at 4 °C. The primary antibodies used were diluted as follows: 1:1000 for LC3B (ab19280, Abcam), 1:500 for p62 (ab109012, Abcam), 1:1000 for BNIP3 (ab109362, Abcam), 1:500 for NLRP3 (Ab283819, Abcam), 1:1000 for IL-1ß (Ab283818, Abcam), 1:1000 for cleaved Gasdermin D (ARG41404, Arigo), 1:1000 for caspase-1 (ARG10644, Arigo), IL-1ß (1:1000; A11945; Ab283818, Abcam), 1:1000 for COX IV (ab202554, Abcam), 1:1000 for alpha Tubulin (ab7291, Abcam) and 1:3000 for β-actin (ab8226, Abcam). Following incubation with horseradish peroxidase-conjugated secondary antibodies (ab6728, ab6721, Abcam), the membranes were developed using an enhanced chemiluminescence detection system. β-actin served as the internal control, detected using an anti-β-actin antibody (ab8226, Abcam). Protein expression levels were quantified based on grayscale values using Image-J software (Version 1.51).

Immunofluorescence staining and confocal microscopy

The hippocampus and temporal cortex of rats were collected and immediately fixed in a 10% buffered formalin solution within 1–2 min of isolation. Following fixation in formalin for 24–48 h, all paraffin-embedded samples were sliced to a thickness of 6–8 μm and placed onto polylysine-coated slides. Paraffin sections were deparaffinized using xylene and graded ethanol. Antigen retrieval was conducted by immersing the sections in 0.01 M citrate buffer (pH 6) in a 95 °C water bath for 45 min. Subsequently, the sections were washed three times with PBS (3 min per wash) after cooling to room temperature. Endogenous peroxidase activity was neutralized by incubating the slides for 15 min with 3% H_2O_2 in the dark. Following an additional three washes with PBS (3 min per wash), the sections were then incubated overnight at 4 °C with primary antibodies targeting for LC3B (1:1000; ab19280, Abcam), p62 (1:500; ab109012, Abcam), for BNIP3 (1:1000; ab109362, Abcam), for TOMM20 (1:1000; ab283317, Abcam), NLRP3 (1:500; Ab283819, Abcam), cleaved Gasdermin D (1:100; ARG41404, arigo); and IL-1ß (1:1000; A11945; Ab283818, Abcam); pMLKL (1:100; ARG43708, Arigo); Cleaved Caspase-3 (1:500; ab32042, Abcam). Sections were subsequently rinsed once more with PBS and then exposed to respective secondary antibodies (1:500 dilutions) conjugated with Alexa Fluor 488 and Alexa Fluor 594, for 45 min at 37 °C. Nuclei were counterstained with DAPI (1 μg/mL) at room temperature for 5 min. Double immunofluorescent labeling of TOMM20 and LC3B was performed to confirm the presence of mitophagy. Images were captured using laser-scanning confocal microscopy (BX53, OLYMPUS).

Enzyme-linked immunosorbent assay (ELISA)

ELISA kits (Cloud-Clone, Wuhan, China) were used to measure the concentrations of IL-1β, IL-18 in the supernatants from brain tissue homogenates of SD rats, following the manufacturer's instructions. The activities were read as the OD at 450 nm.

Statistical analysis

Statistical analyses were conducted using GraphPad Prism 9.5 (GraphPad Software, Inc., La Jola, CA, USA). Quantitative data are presented as mean ± standard error of the mean (SEM). Group comparisons were performed using t-tests for two groups. Multigroup comparisons were conducted using one-way analysis of variance (ANOVA). The level of statistical significance was set to $P < 0.05$.

Data availability

The datasets used and/or analyzed during this study are available from the corresponding author on reasonable request.

Received: 4 July 2024; Accepted: 2 May 2025
Published online: 10 May 2025

References

1. Bejarano, E. & Rodriguez-Navarro, J. A. Autophagy and amino acid metabolism in the brain: implications for epilepsy. *Amino Acids*. **47**, 2113–2126 (2015).
2. Giorgi, F. S., Biagioni, F., Lenzi, P., Frati, A. & Fornai, F. The role of autophagy in epileptogenesis and in epilepsy-induced neuronal alterations. *J. Neural Transm (Vienna)*. **122**, 849–862 (2015).
3. Cao, L. et al. Vitamin E inhibits activated chaperone-mediated autophagy in rats with status epilepticus. *Neuroscience* **161**, 73–77 (2009).
4. Dong, Y. et al. Ascorbic acid ameliorates seizures and brain damage in rats through inhibiting autophagy.
5. Ni, H., Gong, Y., Yan, J. Z. & Zhang, L. L. Autophagy inhibitor 3-methyladenine regulates the expression of LC3, Beclin-1 and ZnTs in rat cerebral cortex following recurrent neonatal seizures. *World J. Emerg. Med.* **1**, 216–223 (2010).
6. Lemasters, J. J. Selective mitochondrial autophagy, or mitophagy, as a targeted defense against oxidative stress, mitochondrial dysfunction, and aging. *Rejuvenation Res.* **8**, 3–5 (2005).
7. Chen, S. D., Chang, A. Y. & Chuang, Y. C. The potential role of mitochondrial dysfunction in seizure-associated cell death in the hippocampus and epileptogenesis. *J. Bioenerg Biomembr.* **42**, 461–465 (2010).
8. Chuang, Y. C., Chang, A. Y., Lin, J. W., Hsu, S. P. & Chan, S. H. Mitochondrial dysfunction and ultrastructural damage in the hippocampus during Kainic acid-induced status epilepticus in the rat. *Epilepsia* **45**, 1202–1209 (2004).
9. Zsurka, G. & Kunz, W. S. Mitochondrial dysfunction in neurological disorders with epileptic phenotypes. *J. Bioenerg Biomembr.* **42**, 443–448 (2010).
10. Chen, H. & Chan, D. C. Mitochondrial dynamics–fusion, fission, movement, and mitophagy–in neurodegenerative diseases. *Hum. Mol. Genet.* **18**, R169–176 (2009).
11. Wani, A. et al. Crocetin promotes clearance of amyloid-β by inducing autophagy via the STK11/LKB1-mediated AMPK pathway. *Autophagy* **17**, 3813–3832 (2021).
12. Wani, A. et al. Alborixin clears amyloid-β by inducing autophagy through PTEN-mediated Inhibition of the AKT pathway. *Autophagy* **15**, 1810–1828 (2019).
13. Wani, A. et al. Neuronal VCP loss of function recapitulates FTLD-TDP pathology. *Cell. Rep.* **36**, 109399 (2021).
14. Liu, J., Liu, W., Li, R. & Yang, H. Mitophagy in Parkinson's disease: from pathogenesis to treatment. *Cells*. **8** (2019).
15. Chen, J. et al. Defective autophagy and mitophagy in Alzheimer's disease: mechanisms and translational implications. *Mol. Neurobiol.* **58**, 5289–5302 (2021).
16. Wu, M. et al. Mitophagy in refractory temporal lobe epilepsy patients with hippocampal sclerosis. *Cell. Mol. Neurobiol.* **38**, 479–486 (2018).
17. Kim, M. J., Yoon, J. H. & Ryu, J. H. Mitophagy: a balance regulator of NLRP3 inflammasome activation. *BMB Rep.* **49**, 529–535 (2016).
18. Zhou, R., Yazdi, A. S., Menu, P. & Tschopp, J. A role for mitochondria in NLRP3 inflammasome activation. *Nature* **469**, 221–225 (2011).
19. Nakahira, K. et al. Autophagy proteins regulate innate immune responses by inhibiting the release of mitochondrial DNA mediated by the NALP3 inflammasome. *Nat. Immunol.* **12**, 222–230 (2011).
20. Iyer, S. S. et al. Mitochondrial cardiolipin is required for Nlrp3 inflammasome activation. *Immunity* **39**, 311–323 (2013).
21. Toldo, S. & Abbate, A. The role of the NLRP3 inflammasome and pyroptosis in cardiovascular diseases. *Nat. Reviews Cardiol.* **21**, 219–237 (2024).
22. Long, J. X. et al. The role of NLRP3 inflammasome-mediated pyroptosis in ischemic stroke and the intervention of traditional Chinese medicine. *Front. Pharmacol.* **14**, 1151196 (2023).
23. Ye, Y. et al. Meisoindigo protects against focal cerebral ischemia-reperfusion injury by inhibiting NLRP3 inflammasome activation and regulating microglia/macrophage polarization via TLR4/NF-κB signaling pathway. *Front. Cell. Neurosci.* **13**, 553 (2019).
24. Atabaki, R., Khaleghzadeh-Ahangar, H., Esmaeili, N. & Mohseni-Moghaddam, P. Role of pyroptosis, a pro-inflammatory programmed cell death, in epilepsy. *Cell. Mol. Neurobiol.* **43**, 1049–1059 (2023).
25. Zhang, X. et al. An explanation of the role of pyroptosis playing in epilepsy. *Int. Immunopharmacol.* **136**, 112386 (2024).
26. Chen, J. et al. Mechanism of NLRP3 inflammasome in epilepsy and related therapeutic agents. *Neuroscience* **546**, 157–177 (2024).
27. Yang, X. et al. Rapamycin attenuates mitochondrial injury and renal tubular cell apoptosis in experimental contrast-induced acute kidney injury in rats. *Biosci. Rep.* **38**. (2018).
28. Lei, R. et al. Mitophagy plays a protective role in iodinated contrast-induced acute renal tubular epithelial cells injury. *Cell. Physiol. Biochem.* **46**, 975–985 (2018).
29. Klionsky, D. J. et al. Guidelines for the use and interpretation of assays for monitoring autophagy (4th edition)(1). *Autophagy* **17**, 1–382 (2021).
30. Mangan, M. S. J. et al. Targeting the NLRP3 inflammasome in inflammatory diseases. *Nat. Rev. Drug Discovery*. **17**, 688 (2018).
31. Miao, R. et al. Gasdermin D permeabilization of mitochondrial inner and outer membranes accelerates and enhances pyroptosis. *Immunity* **56**, 2523–2541e2528 (2023).
32. Sun, Y. et al. A mitophagy sensor PPTC7 controls BNIP3 and NIX degradation to regulate mitochondrial mass. *Mol. Cell.* **84**, 327–344e329 (2024).
33. Thijs, R. D., Surges, R., O'Brien, T. J. & Sander, J. W. Epilepsy in adults. *Lancet (London England)*. **393**, 689–701 (2019).

34. Lévesque, M., Avoli, M. & Bernard, C. Animal models of Temporal lobe epilepsy following systemic chemoconvulsant administration. *J. Neurosci. Methods*. **260**, 45–52 (2016).
35. Concepcion, F. A., Ekstrom, N. A., Khan, M. N., Estes, O. O. & Poolos, N. P. Progressive dysregulation of tau phosphorylation in an animal model of temporal lobe epilepsy. *Neuroscience* **522**, 42–56 (2023).
36. Xia, S. et al. Gasdermin D pore structure reveals preferential release of mature interleukin-1. *Nature* **593**, 607–611 (2021).
37. Hu, Z. Y., Peng, X. Y., Liu, F. & Liu, J. Emulsified isoflurane protects rat heart in situ after regional ischemia and reperfusion. *Fundam Clin. Pharmacol.* **28**, 190–198 (2014).
38. Jin, Y. Z. et al. Effects of acetaldehyde and L-carnitine on morphology and enzyme activity of myocardial mitochondria in rats. *Mol. Biol. Rep.* **41**, 7923–7928 (2014).
39. Klionsky, D. J. et al. Guidelines for the use and interpretation of assays for monitoring autophagy. *Autophagy* **8**, 445–544 (2012).
40. Min, F. et al. Impact of LITAF on mitophagy and neuronal damage in epilepsy via MCL-1 ubiquitination. *CNS Neurosci. Ther.* **31**, e70191 (2025).
41. Gao, Y. et al. GLS2 reduces the occurrence of epilepsy by affecting mitophagy function in mouse hippocampal neurons. *CNS Neurosci. Ther.* **30**, e70036 (2024).
42. Tanida, I., Minematsu-Ikeguchi, N., Ueno, T. & Kominami, E. Lysosomal turnover, but not a cellular level, of endogenous LC3 is a marker for autophagy. *Autophagy* **1**, 84–91 (2005).
43. Lamark, T., Svenning, S. & Johansen, T. Regulation of selective autophagy: the p62/SQSTM1 paradigm. *Essays Biochem.* **61**, 609–624 (2017).
44. Armeli, F., Mengoni, B., Laskin, D. L. & Businaro, R. Interplay among oxidative stress, autophagy, and the endocannabinoid system in neurodegenerative diseases: role of the Nrf2- p62/SQSTM1 pathway and nutraceutical activation. *Curr. Issues. Mol. Biol.* **46**, 6868–6884 (2024).
45. Kumar, A. V., Mills, J. & Lapierre, L. R. Selective autophagy receptor p62/SQSTM1, a pivotal player in stress and aging. *Front. Cell. Dev. Biology*. **10**, 793328 (2022).
46. Danieli, A. & Martens, S. p62-mediated phase separation at the intersection of the ubiquitin-proteasome system and autophagy. *J. Cell Sci.* **131**. (2018).
47. Mazzuferi, M., Kumar, G., Rospo, C. & Kaminski, R. M. Rapid epileptogenesis in the mouse pilocarpine model: video-EEG, pharmacokinetic and histopathological characterization. *Exp. Neurol.* **238**, 156–167 (2012).
48. Yu, J. et al. Inflammasome activation leads to caspase-1-dependent mitochondrial damage and block of mitophagy. *Proc. Natl. Acad. Sci. U.S.A.* **111**, 15514–15519 (2014).
49. Davidson, S. M. et al. Mitochondrial and mitochondrial-independent pathways of myocardial cell death during ischaemia and reperfusion injury. *J. Cell. Mol. Med.* **24**, 3795–3806 (2020).
50. Ding, H. G. et al. Hypercapnia promotes microglial pyroptosis via inhibiting mitophagy in hypoxemic adult rats. *CNS Neurosci. Ther.* **26**, 1134–1146 (2020).
51. Niemi, N. M. et al. PPTC7 maintains mitochondrial protein content by suppressing receptor-mediated mitophagy. *Nat. Commun.* **14**, 6431 (2023).
52. Cavalheiro, E. A. The pilocarpine model of epilepsy. *Ital. J. Neurol. Sci.* **16**, 33–37 (1995).
53. Arshad, M. N. & Naegele, J. R. Induction of temporal lobe epilepsy in mice with pilocarpine. *Bio Protoc.* **10**, e3533 (2020).
54. Racine, R. J. Modification of seizure activity by electrical stimulation. II. Motor seizure. *Electroencephalogr. Clin. Neurophysiol.* **32**, 281–294 (1972).
55. Lu, J. et al. Effects of mild hypothermia on the ROS and expression of caspase-3 mRNA and LC3 of hippocampus nerve cells in rats after cardiopulmonary resuscitation. *World J. Emerg. Med.* **5**, 298–305 (2014).
56. Trushina, E. et al. Defects in mitochondrial dynamics and metabolomic signatures of evolving energetic stress in mouse models of Familial Alzheimer's disease. *PLoS One*. **7**, e32737 (2012).
57. Vanhorebeek, I. et al. Insufficient activation of autophagy allows cellular damage to accumulate in critically ill patients. *J. Clin. Endocrinol. Metab.* **96**, E633–645 (2011).
58. Adlimoghaddam, A. & Albensi, B. C. The nuclear factor kappa B (NF-κB) signaling pathway is involved in ammonia-induced mitochondrial dysfunction. *Mitochondrion* **57**, 63–75 (2021).
59. Fontaine, K. M., Beck, A., Stocker-Wörgötter, E. & Piercey-Normore, M. D. Photobiont relationships and phylogenetic history of Dermatocarpon Luridum Var. Luridum and related Dermatocarpon species. *Plants (Basel Switzerland)*. **1**, 39–60 (2012).

Acknowledgements

This study was supported by the Natural Science Foundation of Fujian Province, China (Grant No. 2021J05075), Joint Funds for the innovation of science and Technology, Fujian province (2023Y9286), Fujian Provincial Natural Science Foundation (2024J011004), Fujian Research and Training Grants for Young and Middle-aged Leaders in Healthcare (2022).

Author contributions

All authors contributed to the study conception and design. Material preparation, data collection and analysis were performed by M.W., X.C., X.C., C.Y., F.W. and Y.L. The first draft of the manuscript was written by M.W. and all authors commented on previous versions of the manuscript. All authors read and approved the final manuscript.

Declarations

Ethics approval

The animal study was approved by the Animal Ethics Committee of Fujian Provincial Hospital, and all experimental procedures were performed according to the National Institutes of Health Guide for the Care and Use of Laboratory Animals. The authors complied with the ARRIVE guidelines.

Competing interests

The authors declare no competing interests.

Additional information

Supplementary Information The online version contains supplementary material available at https://doi.org/10.1038/s41598-025-01087-y.

Correspondence and requests for materials should be addressed to X.C. or X.C.